

NOTE: Knife edge skimming for improved separation of molecular species by the deflector

Sebastian Trippel,^{1,2, a)} Melby Johny,^{1,2, b)} Thomas Kierspel,^{1,2,3, b)} Jolijn Onvlee,¹ Helen Bieker,^{1,2} Hong Ye,^{1,2,3} Terry Mullins,¹ Lars Gumprecht,¹ Karol Długołęcki,¹ and Jochen Küpper^{1,2,3}

¹⁾ Center for Free-Electron Laser Science, Deutsches Elektronen-Synchrotron DESY, Notkestraße 85, 22607 Hamburg, Germany

²⁾ Center for Ultrafast Imaging, Universität of Hamburg, Luruper Chaussee 149, 22761 Hamburg, Germany

³⁾ Department of Physics, Universität Hamburg, Luruper Chaussee 149, 22761 Hamburg, Germany

(Dated: 5 September 2018)

A knife edge for shaping a molecular beam is described to improve the spatial separation of the species in a molecular beam by the electrostatic deflector. The spatial separation of different molecular species from each other as well as from atomic seed gas is improved. The column density of the selected molecular-beam part in the interaction zone, which corresponds to higher signal rates, was enhanced by a factor of 1.5, limited by the virtual source size of the molecular beam.

Molecular-beam methods are important in physical chemistry and molecular physics, as they provide unique opportunities to obtain fundamental insight into mechanisms and dynamics of elementary molecular and chemical processes. Furthermore, industrial applications using molecular beams range from the fabrication of thin films to the production of artificial structures such as quantum wires and dots.

Supersonic expansion of a gas into vacuum provides extreme cooling, in the case of atomic or seeded molecular beams typically from ambient or elevated temperatures down to ~ 1 K¹. This approach is used for a large variety of experiments. In many applications the molecular beam is shaped by skimmers, knife edges, razor blades, slits, slit-skimmers, or gratings to select only the most intense part of the beam^{1–5}. Furthermore, molecular beams can be manipulated by electric and magnetic fields which allow, e. g., the separation of the molecules from a seed gas^{6,7}.

Spatial separation of different species is achieved by the electrostatic deflector^{7–9}. Experiments are in this case typically performed at the edge of the deflected molecular beam to maximize the separation or to reduce the amount of signal originating from the seed gas. However, at this position of the beam profile the column density of molecules is rather low. In this note, we present the combination of a knife edge with the electrostatic deflector, which allows for a better separation of the different species of a molecular beam as well as an increase in column density in the interaction region.

A schematic of the experimental setup is shown in FIG. 1. A pulsed molecular beam was provided by expanding a few millibar of indole and a trace of water in 80 bar of helium through a position-adjustable Even-Lavie valve¹⁰. The valve was operated at a temperature of 110 °C and at a repetition rate of 250 Hz. Two transversely, in X - Y , adjustable conical skimmers (Beam Dynamics, model 50.8 with $\varnothing = 3.0$, model 40.5 with $\varnothing = 1.5$ mm) were placed

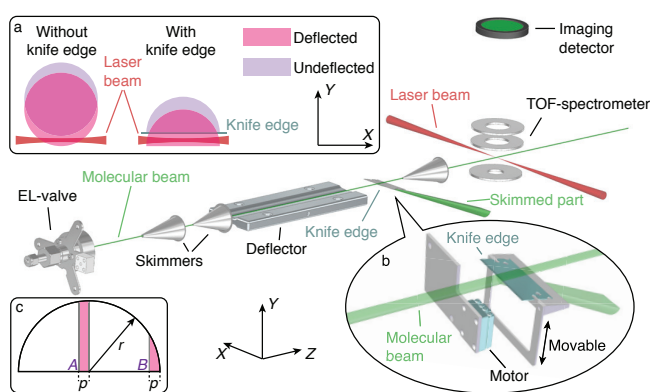


FIG. 1. (Color online) Schematic of the experimental setup and the definition of the coordinate system. a) Sketch of the cross sections of the molecular beam and the laser beam to illustrate the working principle of the knife edge. b) Zoom into the knife edge region, showing the mechanical setup and motorization. c) Definition of the volumes A and B , the beam radius r , and the width p used for the theoretical limit; see text for details.

6.5 cm and 30.2 cm downstream from the nozzle, respectively. The transversely adjustable electrostatic deflector was located 4.4 cm behind the tip of the second skimmer. Using the b-type electrostatic deflector¹¹, the molecular beam was dispersed according to the specific quantum states of the molecular species^{7,9,12}. The vertically, Y , adjustable knife edge was placed 1.3 cm behind the end of the deflector.

For the measurements with knife edge its vertical position was chosen such that the undeflected molecular beam was cut roughly in its center. For the measurements without knife edge it was moved vertically out of the molecular beam. A third, transversely adjustable skimmer (Beam Dynamics, model 50.8 with $\varnothing = 1.5$ mm) was placed 2.5 cm downstream of the front of the knife edge. The molecular beam entered a time of flight mass spectrometer (TOF-MS) centered 17.6 cm downstream of the last skimmer, where the molecules and clusters were strong-field ionized by a laser pulse with a pulse duration of 30 fs, centered at a wavelength of 800 nm, and focused to $\varnothing \approx 50$ μ m. FIG. 1a shows a cross section, in the X - Y

^{a)}sebastian.trippel@cfel.de; <https://www.controlled-molecule-imaging.org>

^{b)}These authors contributed equally.

plane, of the molecular beam to schematically illustrate the working principle of the knife edge. On the left, a molecular beam profile defined by the shape of a round skimmer is depicted. Its deflected part is shown by a vertical shift. On the right, the corresponding profiles are depicted for the case with the knife edge. The laser probes the molecules in the deflected part of the beam, resulting in a higher column density compared to the case without knife edge. FIG. 1b highlights the region of the setup where the knife edge was located. It depicts the knife edge with its holder which was mounted on a motor (SmarAct SLC-1750-S-UHV) which allows to position the knife edge vertically. The molecular beam is indicated by the green cylinder which is cut into halves by the knife edge.

We used the separation of indole and indole-water clusters to demonstrate the advantage of using the knife edge in combination with the electrostatic deflector. FIG. 2a shows the measured vertical density profiles of the undeflected and deflected molecular beam when the knife edge was used. The TOF mass spectrum was gated on specific masses, which corresponded to either parent ions or specific fragments, to obtain each individual profile. The undeflected (0 kV) profile of the signal corresponding to the indole mass of $m = 117$ u is shown in dark blue. All molecules and clusters were deflected downwards when voltages of ± 10 kV were applied to the deflector electrodes, as all quantum states were high-field seeking at the electric field strengths experienced inside the deflector⁷. The deflection profiles for the gates set to the masses of indole, indole(H_2O), indole(H_2O)₂ and (indole)₂ are shown in red, black, green, and orange, respectively. The profiles for indole(H_2O), indole(H_2O)₂, and (indole)₂ were multiplied by a factor of five. The indole(H_2O)₃ cluster was not observed in the mass spectrum. Furthermore, the profile of (indole)₂(H_2O) had the same shape as the one for (indole)₂ and is not shown in the figure. Several edges were observed in the profiles which correspond to various molecules and fragments. Going from left to right, the outermost edge at -1.25 mm is attributed to indole(H_2O) because this cluster showed the largest Stark effect of all molecules and clusters to be considered and was, therefore, deflected the most^{7,12}. The shape of this edge matches the corresponding edge in the indole-ion profile, which confirms that the indole(H_2O) ion was fragmenting to indole ion with a probability of ~ 53 %. The edge at -0.9 mm in the indole-cation signal was attributed to the indole monomer, since indole had the second largest Stark effect. The edge on top of the indole(H_2O) profile at -0.6 mm was produced by indole(H_2O)₂ clusters which fragmented into indole(H_2O) with a probability of ~ 64 %. A better separation of indole(H_2O) from indole and higher clusters was observed in comparison to our previous experiments on this system without the knife edge^{7,12}. Furthermore, the edge for the indole(H_2O)₂ cluster has now been observed for the first time.

FIG. 2b shows the measured deflection profiles for indole corrected by the known fragmentation probabilities to account for the fragmentation for the case with and without knife edge (Knife) and the deflector switched on (red) and off (blue). The profiles for the case without knife edge were shifted by 0.975 mm to the left to match

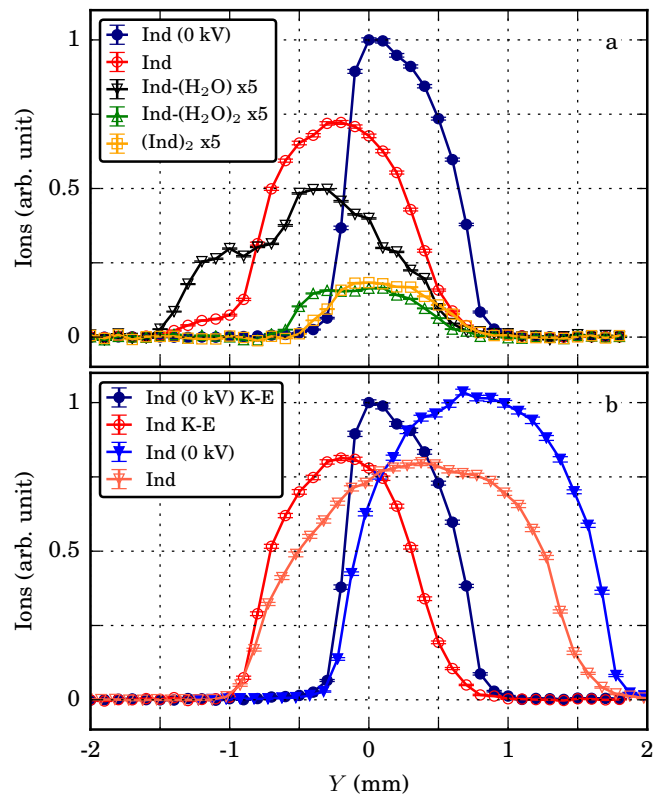


FIG. 2. (Color online) a) Column density profile with knife edge of indole (dark blue), and deflection curves of indole (red open circles), indole(H_2O) (black open triangles), indole(H_2O)₂ (green open triangles), and (indole)₂ (orange open squares). b) Column density profiles with deflector switched off without knife edge (blue triangles), deflector switched off with knife edge (dark blue circles), deflector switched on without knife edge (light red open triangles), and deflector switched on with knife edge (red open circles).

the edges on the left side for a better direct comparison. In both cases – deflector on and off – the left edge was steeper for the measurements with knife edge. This is attributed to the higher column density as a result of the knife edge. Placing the probe laser at -0.7 mm in the deflected profile results in an enhancement factor of $R = 1.5$ at this position. The measured molecular beam diameter of $r = 2$ mm matches exactly the expected radius from geometry arguments assuming a point source for the molecular beam. The distances between the valve and the third skimmer and the interaction region are 53.4 cm and 71 cm, respectively. This results in a magnification factor of $71.0/53.4 = 1.33$, in excellent agreement with the ratio between the measured molecular-beam diameter and the skimmer diameter given by $2.0/1.5 = 1.33$. The deflected part of the molecular beam is, therefore, also expected to be far out of the geometric helium profile. Additional broadening mechanisms for the molecular beam, such as the finite temperature or deviations from a point source are not taken into account. The influence of these contributions to the purity of the molecular beam are beyond the scope of this manuscript.

The maximum enhancement factor R for the increase in column density can be estimated, assuming an uniform

molecular beam emitted from a point source and a uniform deflection force, from the molecular beam radius r in the interaction region and the width of the, for the interaction with the molecules relevant, volume p . For $p \ll r$ the enhancement factor is given by $R = A/B = 3/4\sqrt{2r/p}$, see FIG. 1c. Taking the radius of our measured molecular beam profile of $r = 1.0$ mm and the diameter of the ionization laser $p = 50$ μm resulted in an expected enhancement factor of $R \approx 4.7$. We attribute the reduced experimentally observed enhancement factor of $R = 1.5$ to the following reasons: The experimental molecular beam profile was not completely collimated and, therefore, the edges of the profiles are not infinitely steep. This is ascribed to the finite size of the virtual source, which we estimate to be in the order of 0.6 mm. Due to the finite source size and the geometrical constraints given by the skimmers we furthermore expect it to be advantageous to place the knife edge behind the deflector, compared to using, e. g., a slit-skimmer before the deflector since it decreases the effective virtual source. Secondly, the important volume for the interaction of the molecules with the ionization laser was unknown and might be broader than the measured diameter in intensity. A third contribution to the reduced enhancement is attributed to the fact that the deflector acts as a thick lens for the dispersion of the molecular beam which leads to a softening of the edges. A further contribution could be a misalignment of the knife edge with respect to the propagation direction of the probe laser.

The combination of the knife edge with the electrostatic deflector is of general use for all molecular beam experiments that benefit from a strong separation of molecular species or a strong separation from the seed gas. The presented approach is also especially useful for applications with low count rates or restricted measurement times, e. g., beamtimes at large facilities such as free electron lasers (FELs), synchrotrons, or high-power-laser facilities, where typically only a few days of beamtime are available for the measurements. Furthermore, for probing a collimated molecular beam with $r = 2$ mm by the generally small x-ray beams, e. g., $p = 5$ μm , a theoretical enhancement factor, according to the model described above, of $R > 20$ is obtained. Taking into account the finite virtual source size and the resulting measured reduction of the enhancement factor by about $5/1.5$ leads to an expected enhancement factor of 6 in line with preliminary results from a recent beamtime at the LCLS.

ACKNOWLEDGMENTS

We acknowledge Benjamin Erk and the CAMP team for a significant equipment loan.

Besides DESY, this work has been supported by the excellence cluster “The Hamburg Center for Ultrafast Imaging – Structure, Dynamics and Control of Matter at the Atomic Scale” (CUI, DFG-EXC1074), the European Research Council under the European Union’s Seventh Framework Programme (FP7/2007-2013) through the Consolidator Grant COMOTION (ERC-Küpper-614507), by the European Union’s Horizon 2020 research and innovation program under the Marie Skłodowska-Curie Grant Agreement 641789 “Molecular Electron Dynamics investigated by Intense Fields and Attosecond Pulses” (MEDEA), and by the Helmholtz Association through the Virtual Institute 419 “Dynamic Pathways in Multidimensional Landscapes” and the “Initiative and Networking Fund”. J.O. gratefully acknowledges a fellowship by the Alexander von Humboldt Foundation.

- ¹G. Scoles, ed., *Atomic and molecular beam methods*, Vol. 1 & 2 (Oxford University Press, New York, NY, USA, 1988 & 1992).
- ²W. R. Gentry and C. F. Giese, “High-precision skimmers for supersonic molecular beams,” *Rev. Sci. Instrum.* **46**, 104 (1975).
- ³W. Demtröder, *Laser Spectroscopy 1: Basic Principles* (Springer Verlag, Berlin, 2008).
- ⁴R. Subramanian and M. Sulkes, “Production of a slit skimmer for use in cold supersonic molecular beams,” *Rev. Sci. Instrum.* **79**, 016101 (2008).
- ⁵K. Hornberger, S. Gerlich, P. Haslinger, S. Nimmrichter, and M. Arndt, “Colloquium: Quantum interference of clusters and molecules,” *Rev. Mod. Phys.* **84**, 157 (2012).
- ⁶S. Y. T. van de Meerakker, H. L. Bethlem, N. Vanhaecke, and G. Meijer, “Manipulation and control of molecular beams,” *Chem. Rev.* **112**, 4828 (2012).
- ⁷Y.-P. Chang, D. A. Horke, S. Trippel, and J. Küpper, “Spatially-controlled complex molecules and their applications,” *Int. Rev. Phys. Chem.* **34**, 557 (2015), arXiv:1505.05632 [physics].
- ⁸N. F. Ramsey, *Molecular Beams*, The International Series of Monographs on Physics (Oxford University Press, London, GB, 1956) reprinted in *Oxford Classic Texts in the Physical Sciences* (2005).
- ⁹F. Filsinger, J. Küpper, G. Meijer, L. Holmegaard, J. H. Nielsen, I. Nevo, J. L. Hansen, and H. Stapelfeldt, “Quantum-state selection, alignment, and orientation of large molecules using static electric and laser fields,” *J. Chem. Phys.* **131**, 064309 (2009), arXiv:0903.5413 [physics].
- ¹⁰U. Even, J. Jortner, D. Noy, N. Lavie, and N. Cossart-Magos, “Cooling of large molecules below 1 K and He clusters formation,” *J. Chem. Phys.* **112**, 8068 (2000).
- ¹¹J. S. Kienitz, K. Długolecki, S. Trippel, and J. Küpper, “Improved spatial separation of neutral molecules,” *J. Chem. Phys.* **147**, 024304 (2017), <https://doi.org/10.1063/1.4991479>.
- ¹²S. Trippel, Y.-P. Chang, S. Stern, T. Mullins, L. Holmegaard, and J. Küpper, “Spatial separation of state- and size-selected neutral clusters,” *Phys. Rev. A* **86**, 033202 (2012), arXiv:1208.4935 [physics].